Energy transfer between laser filaments in liquid methanol

B. D. Strycker,* M. Springer, C. Trendafilova, X. Hua, M. Zhi, A. A. Kolomenskii, H. Schroeder, J. Strohaber, H. A. Schuessler, G. W. Kattawar, and A. V. Sokolov

Institute for Quantum Studies and Department of Physics and Astronomy, Texas A&M University, 4242 TAMU, College Station, Texas 77843–4242, USA

**Corresponding author: bstryck2@physics.tamu.edu*

Received June 21, 2011; revised September 2, 2011; accepted September 12, 2011; posted December 7, 2011 (Doc. ID 149612); published December 22, 2011

We demonstrate energy exchange between two filament-forming femtosecond laser beams in liquid methanol. Our results are consistent with those of previous works documenting coupling between filaments in air; in addition, we identify an unreported phenomenon in which the direction of energy exchange oscillates at increments in the relative pulse delay equal to an optical period (2.6 fs). Energy transfer from one filament to another may be used in remote sensing and spectroscopic applications utilizing femtosecond laser filaments in water and air.

OCIS codes: 320.2250, 320.7110.

Femtosecond filamentation occurs when laser beam power reaches a critical value defined by intrinsic properties of the propagating medium; it is a result of the dynamic balance between Kerr self-focusing and defocusing due to low-density plasma [1]. The control of propagating optical filaments has several important applications associated with sophisticated techniques for remote sensing [1,2]. Propagation control methods include prechirping the femtosecond laser pulse [3,4], variable focusing [5,6], and adaptive optics scenarios [7]. Another potential method of controlling the direction or energy content of a propagating filament is energy coupling between two crossed filament-forming femtosecond laser beams. Energy transfer from one filament to another has recently been demonstrated in a number of experiments involving optical filaments in air [8,9]. It has been shown that the direction of energy flow depends on the relative laser pulse delay. In this Letter, we study filament-coupling behavior in transparent liquid bulk media, keeping in mind potential applications to underwater or atmospheric sensing. We observe a coarse time-scale dependence, similar to that described in [8,9], when the pulse delay between the two filament-forming beams is varied over approximately 100 fs. In addition, we find a previously undocumented fine time-scale oscillation in the two-beam energy exchange, which is governed by the relative phase of the filament-forming pulses and has a time-delay period equal to that of the incident radiation (2.6 fs).

An experimental schematic is shown in Fig. 1. We use a Ti:sapphire-based laser system consisting of an oscillator (Mira, Coherent) and an amplifier (Legend, Coherent: 800 nm center wavelength, 35 fs pulse duration, 1 kHz repetition rate, 1 mJ pulse energy). The beam power is controlled by passing through several neutral density filters; the beam is then incident on identical pinholes of 1 mm diameter; we note that diffraction effects from the pinholes may play a role in subsequent filament formation and propagation. One of the two resultant beams is picked off by a D-shaped mirror and directed toward a focusing lens with a 5 cm focal length. The remaining beam is passed through a motorized translation-stage setup (GTS150, ESP301, Newport) and directed parallel to the fixed-path beam. The lateral distance between the two subbeams may be controlled by adjusting the alignment of the fixed-path mirrors; hence, the angle between the interacting beams may also be varied. The interaction region of the two beams is located within the methanol cell (Fig. 1, inset), which is constructed of BK7 glass. The output is then focused by a spherical mirror, projected onto a white screen, and measured with a spectrometer (USB2000, Ocean Optics). Each beam is measured consecutively. We vary the temporal delay between the two pulses by changing the position of the translation stage; the minimal step corresponds to a temporal resolution of 0.33 fs.

In order to make a connection with previous work, we integrate the measured spectra to obtain the total power in each of the output beams. We then calculate the fraction of energy transfer:

$$S = (P_{\text{fixed}} - P_{\text{trans}})/(P_{\text{fixed}} + P_{\text{trans}}), \tag{1}$$

where P_{fixed} and P_{trans} are the power in the fixed-path and translation-stage beams, respectively. Figure 2(a) shows S as a function of the relative delay between the pulses in each beam. For this dataset, the angle between the beams

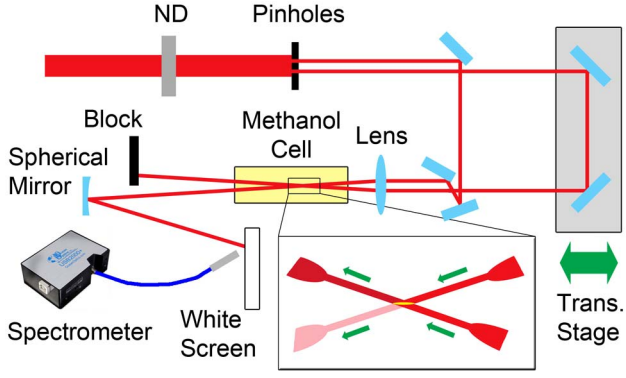

Fig. 1. (Color online) Experimental schematic filter: ND, neutral density. The inset shows the intersection of two filaments involved in energy transfer.

within the methanol sample was 3°, while the group delay dispersion (GDD) at the interaction point was about 7000 fs^2 (positive chirp, with lower frequency components leading the higher ones). The propagation distance within the cell before interaction was 3.5 cm. Formation of single filaments was confirmed for these pulse energy levels upon inspection by adding a fluorescent dye to the methanol sample. The dye was not used for further measurements, which were conducted in pure methanol; formation of single filaments was also verified in the absence of dye by imaging the light exiting the cell with a lens. Filament diameters were measured with knife-edge and fluorescent imaging techniques to be less than 20 μm [10].

In Fig. 2(a), the negative delay corresponds to the translation-stage beam delayed with respect to the fixed-path beam. Notice that at lower input energies, such as 1.20 μJ, the energy transfer goes from high- to low-frequency components, which is consistent with the results in [8]. For higher pulse energy levels, such as 1.52 μJ, the energy transfer changes direction and flows from low to high frequency, which is consistent with the results in [9].

Figure 2(b) shows the difference between the peaks in the energy transfer curve for several pulse energies. Positive values correspond to energy transfer from high to low frequency, while negative values correspond to energy transfer from low to high frequency. It can be seen that the difference between the peaks can be as great as 30%. The direction of energy transfer changes between a pulse energy of 1.3 and 1.4 μJ, while for high pulse energies, the energy transfer again approaches zero. This behavior at high energies is most likely due to the formation of multiple filaments.

The energy transfer curves shown in Fig. 2(a) exhibit a large degree of oscillation; it can be shown that this oscillation is in fact periodic and unique to filament-forming pulses. A typical raw spectral measurement is shown in Fig. 3(a) as a function of relative pulse delay. The total time-delay range in the figure is 30 fs, while the two spectral peaks are located at 830 and 780 nm. A fine time-scale energy transfer, on the order of a 1.3 fs pulse delay, can be seen as oscillations in the spectral intensity. The fine time-scale energy transfer spans the entire spectrum. The spectral components of these datasets were integrated to find the power and energy transfer curves (per Eq. 1) as a function of relative pulse delay. Figure 3(b) shows a

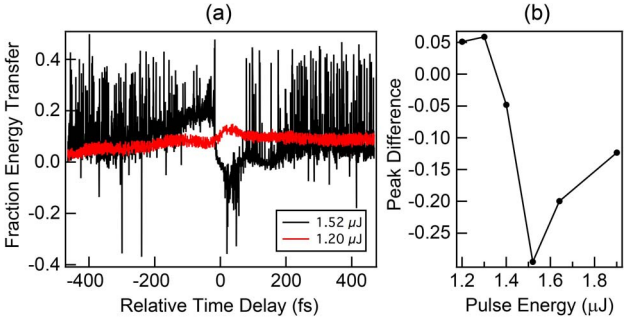

Fig. 2. (Color online) (a) Fraction of energy transfer versus pulse delay for input energies of 1.20 and 1.52 μJ. (b) Difference between fraction of energy transfer curve extrema for several pulse energies.

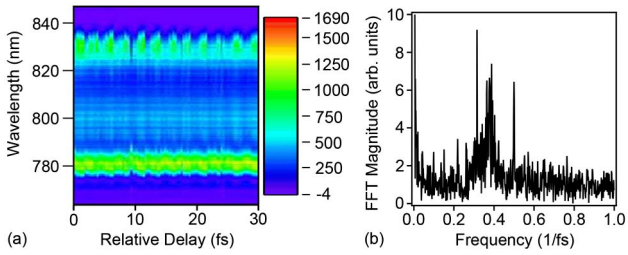

Fig. 3. (Color online) (a) Typical raw spectral measurement of a filament involved in energy transfer in liquid methanol as a function of relative pulse delay. Such raw measurements are spectrally integrated to yield energy transfer curves of Fig. 2(a). (b) Typical FFT of an energy transfer curve for filament-forming, intersecting laser pulses. This FFT peak was completely absent for intersecting pulses that did not form filaments.

typical FFT of an energy transfer curve. The central peak in the FFT at 0.36 fs^{-1} corresponds to the laser carrier frequency. This spectral peak was observed to be entirely absent from energy transfer curves formed from intersecting laser pulses that did not form filaments. This is filament energy exchange on a scale not previously reported.

We next turn to study correlations (or rather anticorrelations) between the output powers for the two beams. Figure 4 shows the energy transfer between the fixed and translation-stage beams corresponding to an energy transfer curve at a fine scale, that is, on a time scale on the order of the period of the incident laser pulses. This fine-scale energy transfer is on top of the larger scale energy transfer shown above and which is consistent with results in [8,9]. In Fig. 4, data points show the measured energy of each pulse, while the red curves show superimposed, out-of-phase sine functions. The fixed and translation-stage pulse energies are shown by circles and triangles (displaced by $2 * 10^4$ detector counts), respectively. It is important to note that, as can be seen in Fig. 4, when one pulse loses energy, the other gains energy, and vice versa.

The presence of fine-scale oscillation was observed for angles between the beams ranging from 1° to 6°, with the observability of the fine-scale oscillation dropping off

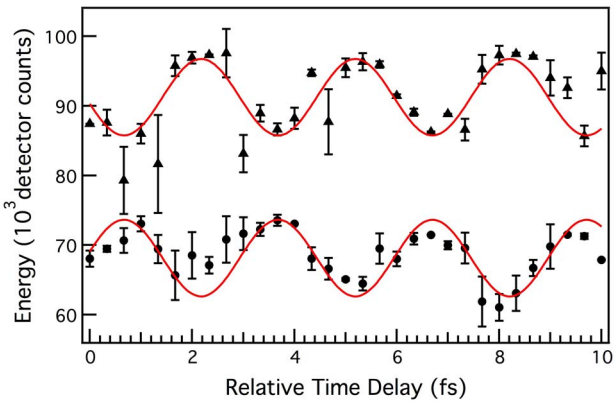

Fig. 4. (Color online) The fine-scale energy transfer between the fixed and translation-stage beams. The measured energies of each pulse are compared to two out-of-phase sine functions. The fixed and translation-stage pulse energies are shown by circles and triangles (displaced by $2 * 10^4$ units), respectively.

above 6°. The extreme sensitivity of the phenomenon to alignment makes analysis of this angular dependence a challenge; a follow-up work detailing this angular dependence is in progress. In addition, we have observed that this fine-scale oscillation in energy transfer between the beams is polarization dependent, and is severely suppressed when the incident beams are orthogonally polarized.

Behavior such as that described above suggests that we have two coherent optical pathways forming a type of a Mach–Zehnder interferometer, where the filament crossing provides the output beam splitter/coupler [11]. The functioning of this beam splitter is possibly similar to the cross-coupling mechanism for a pair of intersecting waveguides. The formation of an intersecting-waveguide structure in a nonlinear Kerr medium has been analyzed by Akhmediev and Ankiewicz [12], who considered linear waves guided by crossed soliton tracks. We find this situation somewhat analogous to our experiment, where the crossed filaments produce a configuration akin to coupled waveguides. In [12], radiation which probes the resultant intersecting-waveguide structure is found to have cross-talk equal to $T_2/T_1 = (\tan\theta/2b)^2$, where T_2 and T_1 are the fractional powers of the two output channels when only one input is present, 2θ is the angle between the beams, and b (termed the soliton amplitude) is approximately equal to λ/d, where λ is the wavelength of the radiation and d is a measure of the diameter of the soliton beam. Taking into account that $T_1 + T_2 = 1$ and solving for T_2 yields $T_2 = 1/[1 + (d \tan\theta/2\lambda)^{-2}]$. If inputs to both channels are present, the interference visibility V is $V = 2\sqrt{T_2(1 - T_2)}$. Taking the wavelength to be 800 nm and the diameters of the filaments in methanol to be less than 20 μm, the interference visibility has a maximum when the angle between the beams is above 9.1°.

Although we observe the said fine-scale oscillation to be most visible at an angle between the beams of about 2° to 4° and falling off above those values, the overall behavior is similar to the prediction of the above rudimentary intersecting-waveguide analysis in that the visibility of the oscillations increases to a maximum value and then decreases with increasing angle.

This research was supported by the Office of Naval Research (contract N00014-08-1-0037), the Defense University Research Initiative Program (contract N00014-08-1-0804), the Robert A. Welch Foundation (grant nos. A-1546 and A-1547), and by the National Science Foundation (grant nos. 0722800, 0555568).

References

1. J. Kasparian, M. Rodriguez, G. Méjean, J. Yu, E. Salmon, H. Wille, R. Bourayou, S. Frey, Y.-B. André, A. Mysyrowicz, R. Sauerbrey, J.-P. Wolf, and L. Wöste, Science **301**, 61 (2003).
2. P. Hemmer, R. B. Miles, P. Polynkin, T. Siebert, A. V. Sokolov, P. Sprangle, and M. O. Scully, Proc. Natl. Acad. Sci. USA **108**, 3130 (2011).
3. G. Méchain, C. D'Amico, Y.-B. André, S. Tzortzakis, M. Franco, B. Prade, A. Mysyrowicz, A. Couairon, E. Salmon, and R. Sauerbrey, Opt. Commun. **247**, 171 (2005).
4. M. Y. Shverdin, S. N. Goda, G. Y. Yin, and S. E. Harris, Opt. Lett. **31**, 1331 (2006).
5. G. Fibich, Y. Sivan, Y. Erlich, E. Louzon, M. Fraenkel, S. Eisenmann, Y. Katzir, and A. Zigler, Opt. Express **14**, 4946 (2006).
6. W. Liu, F. Theberge, J.-F. Daigle, P. T. Simard, S. M. Safiri, Y. Kamali, H. L. Xu, and S. L. Chin, Appl. Phys. B **85**, 55 (2006).
7. J.-F. Daigle, Y. Kamali, M. Châteauneuf, G. Tremblay, F. Théberge, J. Dubois, G. Roy, and S. L. Chin, Appl. Phys. B **97**, 701 (2009).
8. A. C. Bernstein, M. McCormick, G. M. Dyer, J. C. Sanders, and T. Ditmire, Phys. Rev. Lett. **102**, 123902 (2009).
9. Y. Lui, M. Durand, S. Chen, A. Houard, B. Prade, B. Forestier, and A. Mysyrowicz, Phys. Rev. Lett. **105**, 055003 (2010).
10. H. Schroeder and S. L. Chin, Opt. Commun. **234**, 399 (2004).
11. M. Segev and G. Stegeman, Phys. Today **51** (8), 42 (1998).
12. N. Akhmediev and A. Ankiewicz, Opt. Commun. **100**, 186–192 (1993).